

Received August 17, 2019, accepted October 13, 2019, date of publication October 21, 2019, date of current version November 4, 2019.

Digital Object Identifier 10.1109/ACCESS.2019.2948653

# Optimal Color Correction Based on Image Analysis for Color Vision Deficiency

JONGHO CHOI, JUSUN LEE<sup>ID</sup>, HYEONJOON MOON<sup>ID</sup>, SEONG JOON YOO,  
AND DONGIL HAN<sup>ID</sup>, (Member, IEEE)

Department of Computer Science and Engineering, Sejong University, Seoul 05006, South Korea

Corresponding author: Dongil Han (dihan@sejong.ac.kr)

This work was supported in part by the National Research Foundation of Korea Grant funded by the Korean Government under Grant NRF-2017R1D1A1B03028394, and in part by the Institute of Information and Communications Technology Planning and Evaluation (IITP) Grant funded by the Korean Government (MSIT), Development of AI-Convergence Technologies for Smart City Industry Productivity Innovation, under Grant 2019-0-00136.

**ABSTRACT** The primary goal of image color correction is to minimize color confusion for those people who experience deficiencies in their ability to distinguish certain colors. When the colors in a particular image are converted so as to make them perceivable to color vision deficient people, most of the existing methods correct all the colors of the image instead of only the specific colors that are confused. When ordinary people view the images converted using such techniques, they experience a significant difference in perception. To solve this problem, this study investigates the color perception of color vision deficient people through analysis of confused color regions in images and proposes a new method that corrects the minimum number of color regions into optimal colors. For this purpose, the proposed method builds a confusion line database for colors confused by color vision deficient people using the CIEDE2000 color-difference formula and Brettel's method for simulation of color vision deficiency in the offline stage. In the online processing stage, regions are divided through the region growing technique, and the colors in the divided images are compared. When there exist confused colors by color vision deficient people, a method for finding the optimal color is proposed through the confusion line database. Furthermore, this study developed an optimization index to propose a method of finding such optimal colors and validated them through various tests. The excellence of the color correction results of this study was demonstrated based on an objective index as well as on participants' subjective visual perception through comparative experiments with other existing studies.

**INDEX TERMS** Color correction, color vision deficiency, confusion line, image processing, region growing.

## I. INTRODUCTION

With the development of multimedia technology, we can easily access various types of multimedia data, such as reproduced or recorded images, videos, and voices, and these images can now be reproduced and displayed with colors almost identical to their natural appearance due to advanced and high-quality display technology. However, people experiencing color vision deficiency account for approximately 8% of the global population and cannot enjoy or benefit from high-quality multimedia image data to the same degree as others because they do not perceive color the same way and may struggle to accurately discern visual information.

The associate editor coordinating the review of this manuscript and approving it for publication was Shiqi Wang.

The human retina has rod cells that perceive the brightness of the light and has three types of cone cells, L, M, and S, that perceive colors. People with color vision deficiency have a disorder in one of the three types of cone cells and cannot distinguish the color of the wavelength to which each cone cell is most sensitive. Among the people with color-vision deficiency, 26% of those have protanopia, which is a disorder in the L cone cell. 72% of color vision deficient people have deuteranopia, which is a disorder in the M cone cell. and the remaining 2% have tritanopia, which is a disorder in the S cone cell [1].

The spectra for the confusion-line of color-vision deficiencies are very complex. The CIE 1931 color space gives a quite good understanding of this phenomenon using confusion lines [2]. Three primary color-vision deficiencies protanopia (red-blindness), deuteranopia (green-blindness),

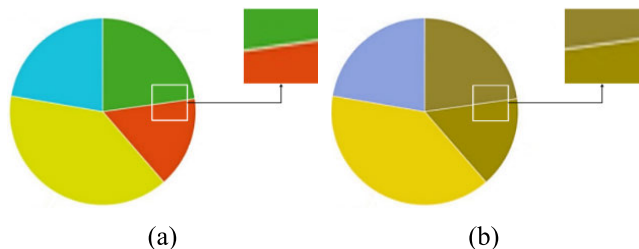


**FIGURE 1.** Image for which color vision deficient people experience altered perception: (a) pie chart as perceived by people with normal vision, (b) pie chart as perceived by people with color vision deficiency.

and tritanopia (blue-blindness) are represented using different arrangements of these confusion lines. All colors in the direction of the confusion lines might be hard to differentiate. The whole spectrum of colors is some way reduced for color vision deficient people. However, substantially color-vision deficiencies have a complex effect on the entire spectrum [3].

Color vision deficiencies may experience disadvantages in the following cases: for example, charts and graphs distinguish detailed information and data through the use of different colors. However, color-vision deficient people have difficulty analyzing charts. This is because different colors are incorrectly perceived as very similar.

Figure 1 shows a typical example of such a perception. In the normal case (a), green and red parts of the pie chart are clearly distinguishable. On the other hand, in color-vision deficiency case (b) same parts of the chart are represented in a similar color, which is indistinguishable.

Leading studies on color vision deficiency include Brettel’s method [4], which simulates the color perception views of color-blind people, and the Machado algorithm [5], which represents the color perception view of color weakness. In addition, confusion lines [6] for defining colors confused by color vision deficient people and the confusion line database [7], [8] have been researched as well. Furthermore, color-correction algorithms [2], [9]–[13] that would help reduce color confusion for color vision deficient people have been researched steadily for many years. Many studies [9], [11], [12] analyzed only the color palette of an image by considering the color perception characteristics of color vision deficient people and modified the color palette itself, thus offering the advantage of low cost. As a result, color vision deficient people can distinguish colors that they previously could not see. The result of the generally used Daltonization technique [9] is shown in figure 2.

A few studies [14]–[16] propose algorithms considering the viewpoints of both color vision deficient people as well as those with normal vision. Shen *et al.* [14] use an extra display channel of stereoscopic display that allows color vision deficient and normal vision audiences to share the same visual contents. Tanaka *et al.* [16] consider the optimization problem concerning lightness modification for protanopia and deuteranopia.

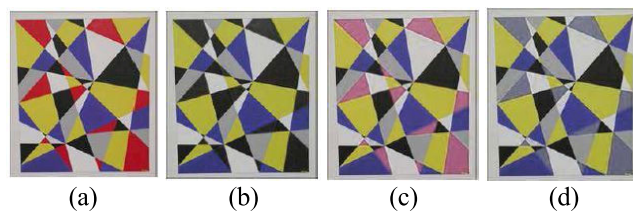


**FIGURE 2.** Example of daltonization: (a) perception by people with normal vision, (b) perception by color vision deficient people, (c) perception of corrected image by people with normal vision, (d) perception of corrected image by color vision deficient people.

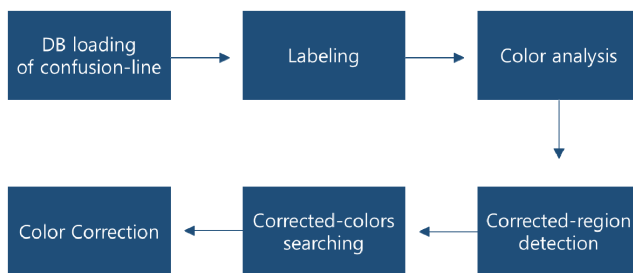


**FIGURE 3.** Block diagram of the optimal color-correction method.

Besides the image-correction method, algorithms for image segmentation [17]–[19] also exist in image analysis. The image segmentation method of [18] divides an image into regions by the local threshold of objects through object extraction. The method of [19] uses the Reversible Jump Markov Chain Monte Carlo (RJMCMC) for the region segmentation of color images. This method clearly divides sections according to natural colors in images.

In this study, the method of dividing into multiple areas is suitable and unlike the existing method, we perform labeling based on color and analyze the areas classified by color. The proposed method performs image segmentation through region growing [21] using the hue value of pixels so that a confusion line database can be applied, thereby detecting confusing colors in images and selecting the regions to be corrected using pixel data and the confusion line database. This process helps determine whether to correct the colors in the image or the segmented sections in the image.

Once the analysis step is completed, the optimized colors of the regions to be corrected in the analyzed image are found and corrected. From the viewpoint of those who are colorblind, the corrected color obtained from the correction process is a color that is not confused with other color groups, and it becomes a color that is easiest to distinguish from other color groups in the image.

## II. OPTIMAL COLOR CORRECTION METHOD

The optimal color correction method is as shown in figure 3. Confusion-line databases are generated by the type of color-vision deficiency on the off-line. We load the confusion-line databases at the beginning for real-time processing. First, images are inputted and converted to HSV (Hue-saturation-value) color space. It generates a histogram based on hue,

and it extracts peak points from this data. It sets hue value of peak point to seed point and it performs labeling. Then it analyzes whether the color exists on a confusion-line based on the color value within a labeled area. It detects areas if it's on the same line of confusion-line. Based on these criteria, color-correction is performed on the optimized color area taking in consideration both normal and color-vision deficiencies.

**A. OFFLINE COFUSION-LINE DATABASE**

In this study, a confusion line database is constructed in advance during the offline stage before performing the optimal color correction. A confusion line database refers to a database constructed by grouping colors confused by color vision deficient people among the colors in a color space such as RGB or CIE L\*a\*b\* [22]. We use the CIE 1931 tristimulus values of the reference white under the illumination. This transforms the RGB color space to XYZ color space and converts it to L\*a\*b\* color space using the extracted XYZ [2] values. According to the related research that human color perception is nonlinear, L\*a\*b\* color space has a nonlinear relationship with the wavelength of actual light. In addition, the two different colored distances in L\*a\*b\* space are designed to be proportional to the differences in colors felt by humans.

In CIE L\*a\*b\* color space, the L\* value indicates brightness. Its range consists of 0 to 100. If the L\* value is 0, it is expressed in black, and it is described as white if the value of L\* is 100. a\* exists on red-green space, and b\* stands for the yellow-blue region. In theory, there are no maximum values of a\* and b\*, they are usually numbered from -128 to 128. Then we normalize these from -100 to 100. If a\* is negative, it is close to the green, if it is positive, it is close to red/violet.

In this paper, the proposed color-correction approach by the group rather than by pixel, and as shown in floor function equation (1), the channels of the L\*a\*b\* space are divided into boxes containing 5, 13, and 13 values, respectively to perform normalization with approximate values. For example, if CIE L\*a\*b\* is (70.66, -9.68, 45.32), the location of the discretized value is computed by (14.132, -0.7446, 3.486), and the actual box-index is rounded to specify (14, -1, 3). The L\*index value has a discretized integer value between 0 at the minimum and 20 at the maximum, and a\*index and b\*index values have discretized values between +8 and -9. In this case, the L\*a\*b\* space is quantized into 21\*17\*17 = 6,069 boxes, and there can be up to 6,069 discretized representative colors. However, there are so many invisible colors in this color space. So, the actual visible area lies in the center of this color space that is expressed in only 1,475 representative colors. The discretization result after the above process is shown in figure 4, which used the CIE L\*a\*b\* color space.

$$\begin{aligned}
 L^*_{index} &= \lfloor L^*/5 \rfloor \quad (0 \leq L^* \leq 100) \\
 a^*_{index} &= \lfloor a^*/13 \rfloor \quad (-100 \leq a^* \leq 100) \\
 b^*_{index} &= \lfloor b^*/13 \rfloor \quad (-100 \leq b^* \leq 100)
 \end{aligned} \tag{1}$$

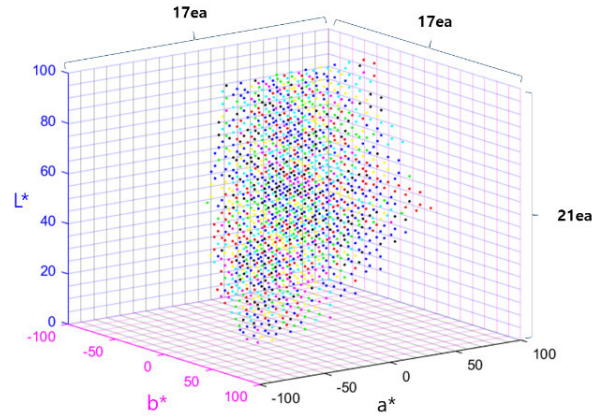


**FIGURE 4. Visualization result of representative colors.**

The confusion between representative colors is tested by simulating discretized representative colors through Brettel's method [4]. Color confusion was defined as when the difference between the simulated colors through the CIEDE2000 [23] color difference formula is lower than the threshold. In this study, the threshold was set to 3 for the construction of the confusion line database.

When this process is applied to every representative color, each representative color will have a corresponding list of colors that are often confused with the representative color.

K-means [24] and SVM [25] were commonly used as traditional methods for grouping. The proposed confusion-line model is a situation in which each representative color should be included in multiple groups. However, the previous clustering methods such as K-means and SVM only group with similar colors and they generate small number of groups. Therefore, it was concluded that the confusion-line model was unsuitable for the use of the K-means and SVM methods.

In this research, grouping was carried out using thresholds and discretized colors that belong to multiple confusion line groups at the same time. The representative colors for color vision deficiencies can be expressed in 1,475 groups. Confusion-line database is generated within these groups. Confusion lines refer to ranges that do not distinguish different colors based on color-vision deficiency and recognize them as similar colors. The color difference is computed as CIEDE2000 (Color differences formula) and this score is defined as the "ΔE<sub>00</sub>" value. First, it is going to simulate images that are viewed by color-vision deficiency. ΔE<sub>00</sub> values between these images are calculated and then it determines whether a grouping is based on the threshold value.

Figure 5 shows the grouping process between (color 597, color 718, color 998) based on representative color 717. Its group has 30 colors, including itself. (color 717, color 597, color 998) represents the (1<sup>st</sup>, 2<sup>nd</sup>, 30<sup>th</sup>) color within this group. And color 718 shows the 718<sup>th</sup> representative color of figure 7. If you look at the processing, firstly colors (717, 597, 718, 998) are converted by color-vision deficiency

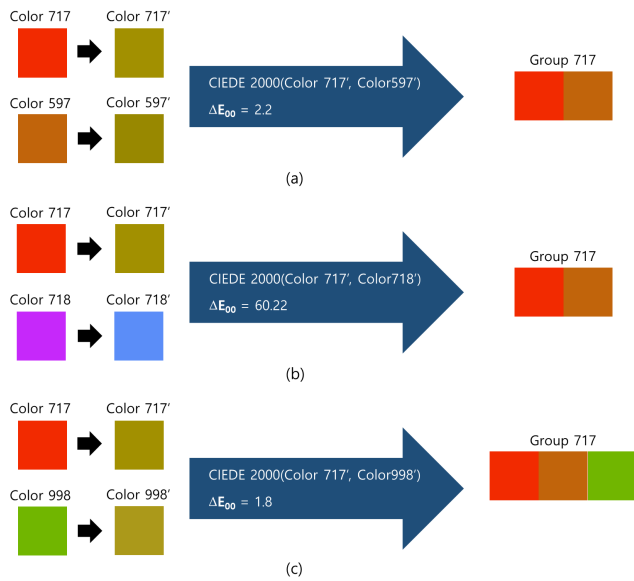


**FIGURE 5.** Examples of representative color grouping: (a) Color 717 and Color 597 are converted to CVD simulated versions 717' and 597' respectively. Then  $\Delta E_{00}$  is computed for these simulated versions. Since it is lower than the set threshold 3, the original Color 597 is added to the confusion line group of Color 717. (b)  $\Delta E_{00}$  for CVD simulated versions of Color 717 and Color 718 is 6.8 that is higher than the threshold, so Color 718 is not added to the group. (c)  $\Delta E_{00}$  for CVD simulated versions of Color 717 and Color 998 is less than the threshold, so Color 998 is added to the group.

simulation. These converted colors are expressed by colors (717', 597', 718', 998'). Then the difference ( $\Delta E_{00}$ ) between colors is calculated using the CIEDE 2000 method. The difference between color 717' and color 597' is 2.2, the difference between color 717' and Color 718' is 6.8, and the difference between color 717' and Color 998' is 1.8. In this study, we set an experimental threshold of 3 for grouping. As a result, only color 597 and color 998 are grouped with representative color 717. Thus, the 717<sup>th</sup> representative color is grouped with 27 other representative colors. The other representative colors with which the 717<sup>th</sup> representative color is grouped corresponded to (717, 597, 609, 621, ..., 988, and 998). Since, the representative color 717 is on the same confusion line as its group members, it will also be added to the confusion line groups of the other member representative colors e.g. Color 597 and Color 609.

The group result is visualized in figure 6. The x-axis means a representative color for color-vision deficiency, which consists of 1,475 representative colors. The confusing colors for representative colors are shown as pixels along the y-axis. Since each color is compared with all the colors in discretized representative colors, it can be confused with multiple colors (i.e.  $\Delta E_{00}$  is less than a threshold), so each color may be part of multiple groups. The height of the y-axis refers to the number of confusing colors and describes the confusing colors on the graph sequentially.

An expanded image is shown in figure 7 to convey a clearer view of the grouping result. Within figure 6(b), the red box is enlarged. The colors in group 715 in figure 7(a) consist

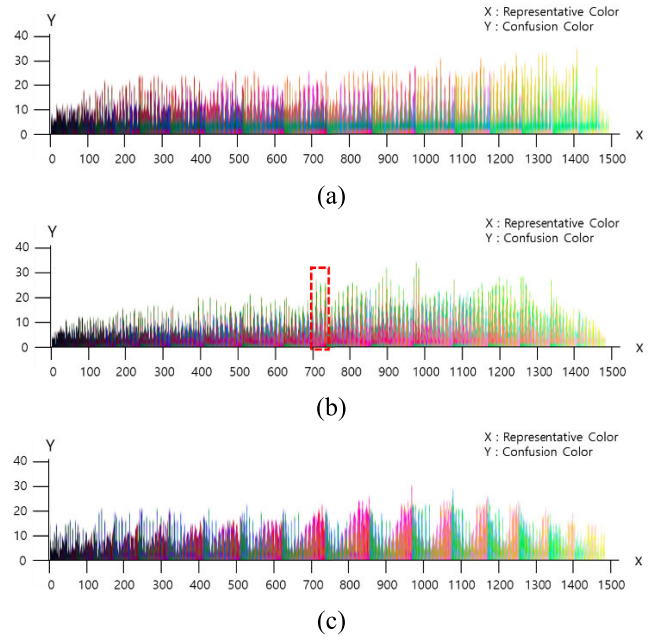


**FIGURE 6.** Visualization result of confusion line database: (a) confusion line database for people with protanopia, (b) confusion line database for people with deuteranopia, and (c) confusion line database for people with tritanopia.

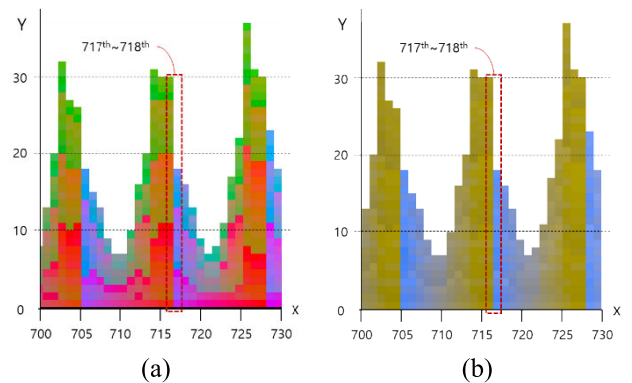


**FIGURE 7.** Enlarged image of the confusion line database visualization result of people with deuteranopia: (a) Colors perceived by people with normal vision, (b) colors perceived by color vision deficient people.

of red and green. In figure 7(b), that shows a simulation from the viewpoint of people with deuteranopia, the colors appear almost identical. Even though the colors in adjacent groups appear similar, their color difference is greater than the defined threshold value.

In the case of an ordinary grouping process, the number of groups created is smaller than the number of original colors. In this study, however, 1,475 confusion-line groups that are confused by color vision deficient people were created using 1,475 representative colors. In other words, all colors confused with specific representative colors are included in the confusion line list of the corresponding representative color. If the confusion line database is constructed in this way, the same representative color belongs to multiple groups at

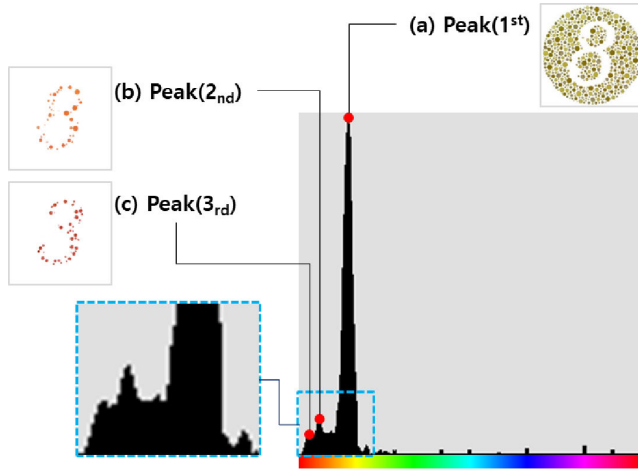


FIGURE 8. Samples of extracted seed-points using Ishihara table (number 8) images.

the same time. It enables easy to search for the confusing colors during online processing.

**B. ONLINE COLOR CORRECTION**

1) DB LOADING OF CONFUSION LINE

The first step of image correction involves loading the confusion line database, which will be used to analyze the colors in the image. As described above, a confusion line database is a list of data. Thus, color optimization and correction are prepared through the simple loading of the database. Furthermore, when the user specifies his or her type of vision deficiency, the confusion line database aligned with that specific deficiency type is used.

2) LABELING

In this paper, regions are divided through the region growing method [21]. The region growing method is a region-based segmentation method. Images are divided into small regions, and similar regions are combined by calculating color sense or brightness differences then the final image is divided into regions. In this study, the pixels with high-frequency colors in the image were specified as the seed point in the beginning stage, and the regions were expanded by attaching similar pixels among the pixels near the seed point to the seed point, and the regions with the same color in the entire image are segmented.

We extract the peak-points on the hue-histogram as shown in the figure 8. On the histogram, the x-axis represents a hue value, and the y-axis represents a frequency of a color distribution existing in the image. The peak (a) of the figure 8 shows the major distribution value in the image, and the peak (c) of the figure 8 illustrates the 3<sup>rd</sup> largest distribution value in the image.

Figure 9 shows the process of expanding the area in 8-directions relative to the seed point. This distinguishes between red and green areas and labels them by determining whether they are of similar color within neighborhood pixels.

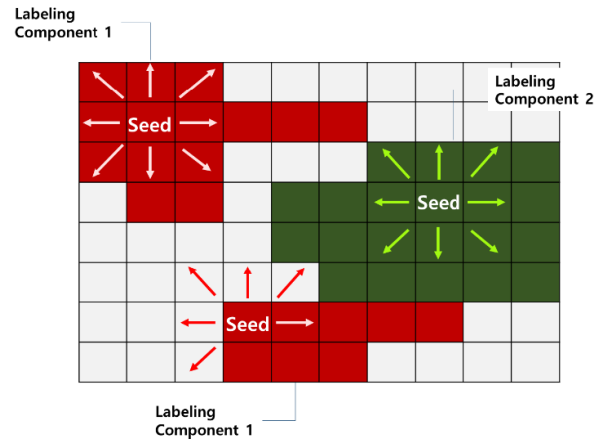


FIGURE 9. Visualization of region growing method.

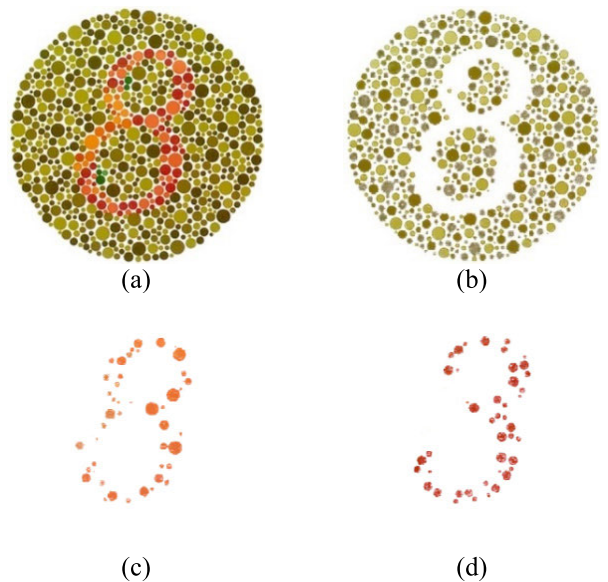


FIGURE 10. Sample of segmentation result: (a) original, (b) labeling component 1, (c) labeling component 2, and (d) labeling component 3.

Because the hue value is used as the information for the seed point, the region of the seed point is expanded for similar colors. An example of the region growing performed in this research is shown in figure 10.

The region segmentation required for object recognition requires a more precise region growing technique, but in this study, the parts with similar color information are regarded as the same region. Besides, separated regions are regarded as the same region if their colors are similar.

3) COLOR ANALYSIS

To avoid confusing the corrected colors with other colors while in the process of correcting colors in the image, the colors in every region in the image were analyzed and all the confusion lines believed to exist in the image were removed from the list of corrected colors. For example, assuming that there are only two colors in the image, the two confusion lines

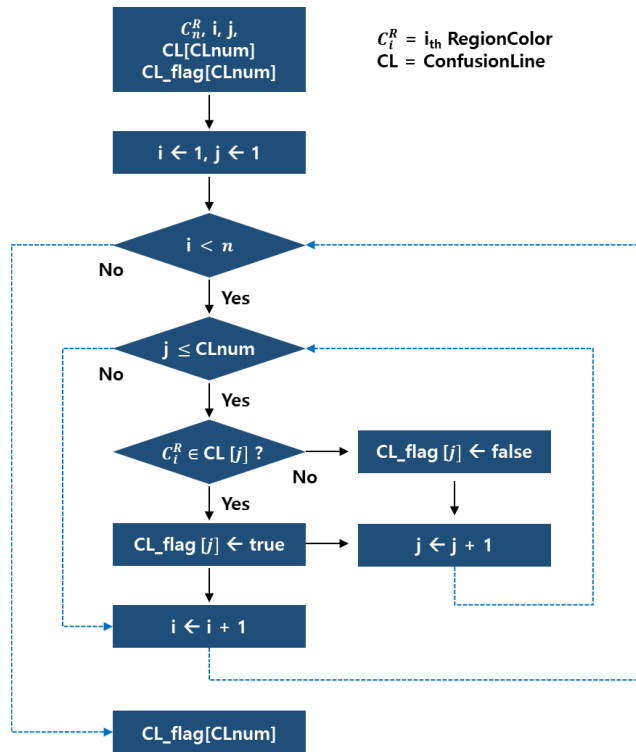


FIGURE 11. Flowchart of the confusion-line list eliminator.

of representative colors as well as all the confusion lines that contain the two colors are removed from the list of colors to be corrected. Furthermore, this process is carried out until there is no confusion among any color.

This process is shown as a flowchart in figure 11. To explain the variables in this flowchart,  $C_i^R$  is the concept of color including RGB and CIE  $L^*a^*b^*$  that exist in the  $i^{th}$  region in the image.  $CL[j]$  stands for the inside of  $j^{th}$  group confusion line DB in figure 6,  $n$  is the number of regions inside the image and  $CLnum$  indicates 1,475, which is the number of confusion lines and the number of representative colors. The value of  $CL\_flag$  is determined by the presence of ConfusionLines' in the image. If the value of  $CL\_flag == true$ , the corresponding confusion line exists in the image which means the color inside  $CL[j]$  DB was included in the image, and when  $CL\_flag == false$ , the corresponding confusion line does not exist in the image hence, no color is confused in the image. The process of analyzing the confusion line in the image makes it possible to select the corrected color in the confusion line database excluding confusion lines that already exist when the corrected color is selected, thus removing the possibility of re-correction.

An example of image correction without this process is shown in figure 12. From the viewpoint of people with normal vision, the image segmentation result is the division of six regions, which have red, sky blue, green, yellow, purple, and blue colors from left to right. From the viewpoint of those with color vision deficiency, the colors are yellow, sky blue, yellow, bright yellow, light blue, and blue from left to right.

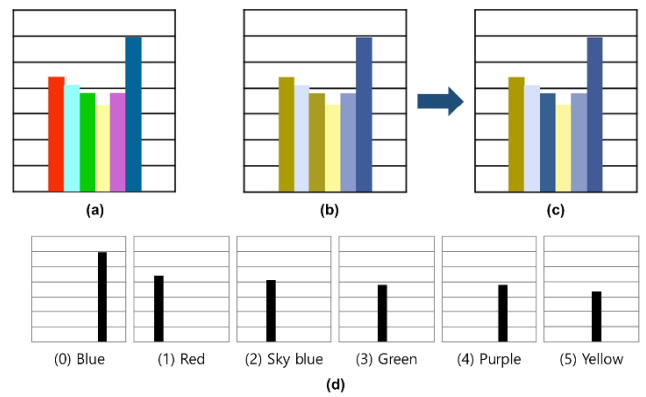


FIGURE 12. Example images that require re-correction: (a) perception by people with normal vision, (b) perception by color vision deficient people, (c) example of incorrect correction, and (d) example of segmented regions.

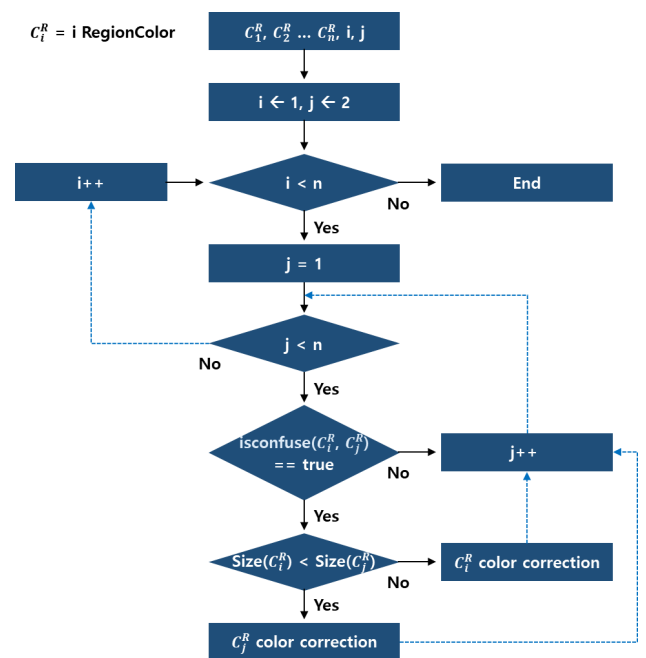


FIGURE 13. Flowchart for specifying the region to be corrected.

In this case, if the green color, which is the region 3 in figure 12(d), is corrected to blue to avoid confusion with red, it could be confused again with the other blue region, which is the region 0 in figure 12(d), during the correction process. An example of this is shown in figure 12(c). The colors confused with yellow before correction (region 1 and region 3) are corrected into yellow and blue, and it appears to be a proper correction with no confusion, but it can be confused again with the blue region (region 0). In this study, this problem is prevented at the source by removing all of the representative color confusion lines of the colors that are present.

#### 4) CORRECTED-REGION DETECTION

Figure 13 shows a flowchart of the process for specifying regions to be corrected. Here, specifying regions means an

TABLE 1. Definition of isConfuse().

```

1: isConfuse( $C_i^R, C_j^R$ )
2: Confusion_Threshold  $\leftarrow$  15
2: box_Color; Lab  $\leftarrow$  boxindex( $C_i^R$ )
3: box_Color; Lab  $\leftarrow$  boxindex( $C_j^R$ )

4: if (equalConfusionLine(box_Color; Lab, box_Color; Lab) == true) then
5:     Color; Lab  $\leftarrow$   $C_i^R$ 
6:     Color; Lab  $\leftarrow$   $C_j^R$ 

7:     if ( $\Delta E_{00}$ (Color; Lab, Color; Lab) > Confusion_Threshold) then
8:         return true
9:     else
10:        return false
11:    end if
12: else
13:    return false
14: end if
    
```

area that doesn't discriminate colors based on the color-vision deficiency. First, it determines whether colors are distinguishable based on representative color and confusion-line database by each zone. After comparing the size of the area if it is on the same confusion-line, the color of the small area is then converted to a different color.

The method of specifying the regions to be corrected consists of comparing the size between regions and checking  $isConfuse(C_i^R, C_j^R)$  to judge the possibility of confusion between regions as shown in table 1. Once segmentation in the image is completed through region growing,  $isConfuse(C_i^R, C_j^R)$  compares the colors of  $C_i^R$  and  $C_j^R$ , which are the list of colors representing each segmented region, and outputs the result of confusion (true or false). If confusion is true, the distributions of two colors in the image are compared, and the color with a smaller area is corrected to minimize the color-corrected regions.

Using figure 14 and table 2, this process can be explained as follows. To compare RGB = (182, 176, 88), which is the color corresponding to the number 16 region with RGB = (215, 127, 77), which is the color corresponding to the current background region, they are changed to the CIE L\*a\*b\* color space first and then converted to Box<sub>index</sub>. It is verified whether the colors exist in the same confusion line through comparison of the converted to Box<sub>index</sub> (14, -1, 3) and (12, 2, 3) with the corresponding confusion line database.

If they exist in the same confusion line, it is classified as a region to be corrected because it is regarded as a color confused by color vision deficient people. As mentioned above, when 1,475 confusion lines are created using 1,475 representative colors, it becomes very easy to find the confusion line database. In other words, the confusing colors can be determined very easily by selecting a random color between two colors under consideration, finding the representative colors, and searching the corresponding list.

5) SEARCHING OPTIMAL COLOR

For optimal color correction, an index related to the valid processing of color correction should be calculated. Being

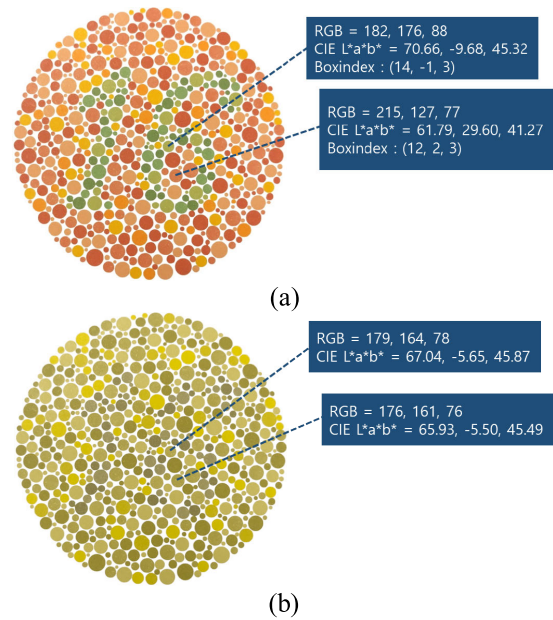


FIGURE 14. Example calculation process to search confusing colors: (a) in case of normal vision, (b) in case of color vision deficiency.

TABLE 2. Example of is Confuse function.

Symbol	$\Delta E_{00}$	Result of isConfuse( $C_i^R, C_j^R$ )
Normal vision	28.74	True
Color vision deficiency	0.90	

“valid” means the color regions that previously caused confusion for people with color vision deficiency are now distinguishable and the converted colors are very similar to the pre-corrected colors from the viewpoint of those with normal vision. A new measure was proposed in this study because SSIM [26] and PSNR [27], which have been used frequently in existing image processing studies, cannot be regarded as proper measures for comparing confused color images. The new color optimization method analyzes images but also considers the perspectives of both color vision deficient people and those with normal vision. In other words, the proposed method compares the color differences within segmented color regions before and after color correction while simultaneously comparing the color differences of segmented color regions in images simulating the viewpoint of color vision deficient people using Brettel’s method [4]. To accurately represent the differences between colors, the CIEDE2000 color-difference formula [23] provided by CIE is used. This color difference formula expresses the difference as  $\Delta E_{00}$  and determines the differences between colors using CIE L\*a\*b\* [22] and HSV [28] color spaces as accurately as possible.

An example calculation process of the image optimization method is shown in figure 15 and table 3 below. The colors of two regions that were determined to be confusing after image analysis were defined as  $C_1^R$  and  $C_2^R$ , and respectively

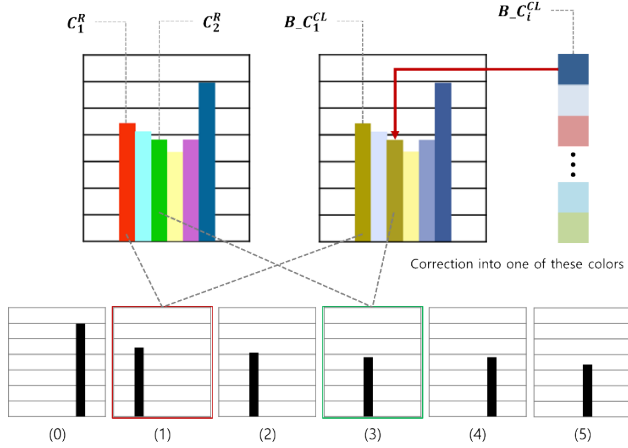


FIGURE 15. Image correction process example.

representative colors to newly corrected color at the position of  $C_2^R$  is defined as  $C_i^{CL}$ . The regions calculated through the region growing method are sorted in descending order by calculating the color distribution histogram in the image. The color with a larger region becomes  $C_1^R$ , and the color with a smaller region becomes  $C_2^R$ .

The calculation of the color difference between  $C_2^R$  and  $C_i^{CL}$  to determine the color difference of perception by people with normal vision after correction is defined as  $ColorDiff_{NORMAL}$ , which is expressed in Eq. (2). Furthermore, the calculation of the color difference between  $B_C1^R$  and  $B_Ci^{CL}$  which are Brettel simulations for  $C_1^R$  and  $C_i^{CL}$ , respectively, to determine the color difference perceived by color vision deficient people after correction is defined as  $ColorDiff_{CVD}$ , which is expressed in Eq. (3). Here,  $C_i^{CL}$  targets the colors remaining after excluding the confusion lines determined to exist among the number of representative colors,  $CLnum$  ( $= 1,475$ ). In this study, the index of the representative color,  $O_{index}$ , that can most optimally perform correction is found by comparing every color that exists in  $C_i^{CL}$  and the color difference before and after the Brettel simulation of  $C_1^R$  and  $C_2^R$ , and then correction is performed to the corresponding color as  $O_{index}C_{O_{index}}^{CL}$ . This process is repeated for the other confusing color regions.

$$ColorDiff_{NORMAL} = \Delta E_{00}(C_2^R, C_i^{CL}) \quad (2)$$

$$ColorDiff_{CVD} = \Delta E_{00}(B_C1^R, B_Ci^{CL}) \quad (3)$$

$$Diff_{CVD} = \sqrt{(ColorDiff_{CVD} - Color_{val})^2} \quad (4)$$

$$Diff_{Color} = Diff_{CVD} + ColorDiff_{NORMAL} \quad (5)$$

$$O_{index} = \underset{i}{\operatorname{argmin}}(Diff_{Color}) \times \{i | CL\_flag[i] \equiv \text{false and } i \in CLnum\} \quad (6)$$

The optimization equation is shown in Eq. (6). If  $ColorDiff_{CVD}$  is too large, the color is corrected to an extraordinary color and creates a heightened difference in perception for those with normal vision. If this

TABLE 3. Color optimization algorithm.

```

1:  $i \leftarrow 0, \min \leftarrow 512, Color_{val} \leftarrow 25, CLnum \leftarrow 1,475$ 
2:  $Type \leftarrow \text{Type of CVD}$ 

3: for ( $i < CLnum$ )
4:   //Identification of same confusion-line
5:   if ( $CL\_flag[i] == \text{false}$ ) then

6:     // Calculation of color distance based on normal
7:      $ColorDiff_{NORMAL} \leftarrow \Delta E_{00}(C_2^R, C_i^{CL})$ 
8:     // Calculation of color distance based on CVD
9:      $B_C1^R \leftarrow \text{Brettel\_Conv}(C_1^R, Type)$ 
10:     $B_Ci^{CL} \leftarrow \text{Brettel\_Conv}(C_i^{CL}, Type)$ 
11:     $ColorDiff_{CVD} \leftarrow \Delta E_{00}(B_C1^R, B_Ci^{CL})$ 
12:     $Diff_{CVD} \leftarrow \text{sqrt}((ColorDiff_{CVD} - Color_{val})^2)$ 
13:    // Calculation of optimized color
14:     $Diff_{color} \leftarrow Diff_{CVD} + ColorDiff_{NORMAL}$ 
15:  else
16:     $i++$ 
17:    continue
18:  end if
19:  // Extraction of the minimum difference
20:  if ( $Diff_{color} < \min$ ) then
21:     $\min \leftarrow Diff_{color}$ 
22:     $O_{index} \leftarrow i$ 
23:  end if
24:   $i++$ 
25: end for
26: return  $O_{index}$ 

1_1: Brettel_Conv( $L^*a^*b^*, Type$  of CVD)

1_2: // Color conversion from Lab to RGB
1_3:  $RGB \leftarrow \text{Lab\_to\_RGB}(L^*a^*b^*)$ 

1_4: if ( $Type$  of CVD == protan) then // protanopia
1_5:   $Br\_RGB \leftarrow \text{Brettel}(RGB, p)$ 
1_6: else if ( $Type$  of CVD == deutan) then // deutanopia
1_7:   $Br\_RGB \leftarrow \text{Brettel}(RGB, d)$ 
1_8: else if ( $Type$  of CVD == tritan) then // tritanopia
1_9:   $Br\_RGB \leftarrow \text{Brettel}(RGB, t)$ 
1_10: end if

1_11: // Color conversion from RGB to Lab
1_12:  $Br\_Lab \leftarrow \text{RGB\_to\_Lab}(Br\_RGB)$ 

1_13: return  $Br\_Lab$ 

```

value is too small, then those viewers with color vision deficiency will struggle to distinguish certain colors. Thus, the size of this value is adjusted by the constant color difference  $Color_{val}$ . The  $Color_{val}$  value may vary depending on color-vision deficiencies, and this value indicates the degree to which the colors are distinguished. In equation (4), we conducted an experiment by setting the  $Color_{val}$  value to 25. As we can see in the images below, if we increase the value for  $Color_{val}$  the output color is more distinguishable for color vision deficient people but increasing it too much may cause output image get too far from the original image for normal people. Vice versa, if we decrease the value for  $Color_{val}$ , the output image will be closer to original for normal people but it will be difficult to distinguish for color vision deficient people.

Besides,  $ColorDiff_{NORMAL}$  is also considered because a smaller color difference of the converted color experienced by those with normal vision is better. Therefore, this study's



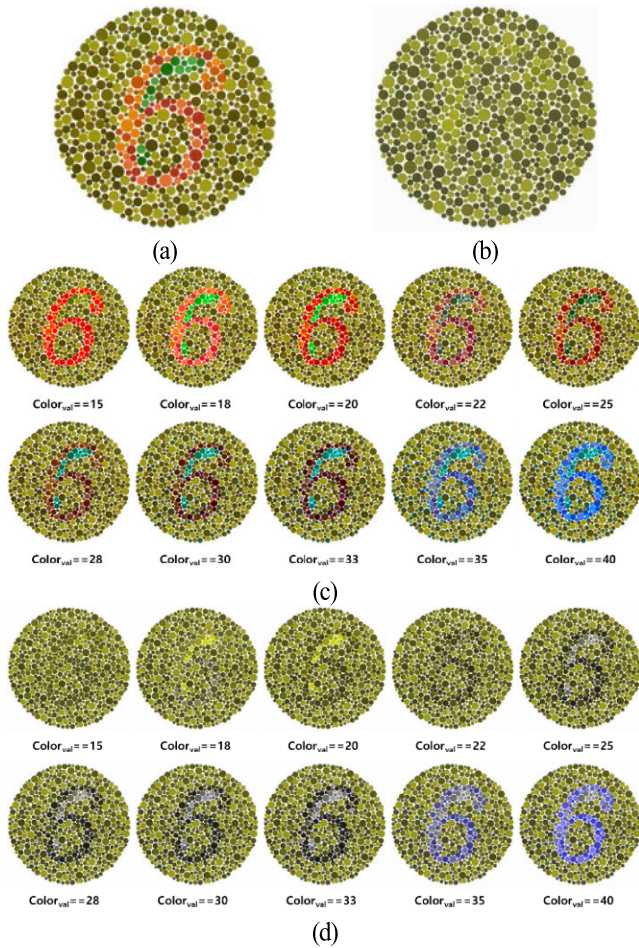


**FIGURE 16.** Experimental results for  $Color_{val}$ : (a) original image, (b) image felt by color-vision deficiency(deuteranopia) based on the original image, (c) images felt by normal people, (d) images felt by color-vision deficiencies.

index was set in such a manner to find the color that minimizes color change for people with normal vision while allowing color vision deficient people to sufficiently perceive the converted colors.

In equation (4) we want to minimize the root mean square error between  $ColorDiff_{CVD}$  and constant  $Color_{val}$  such that  $ColorDiff_{CVD}$  value is almost identical to the  $Color_{val}$ . As a result,  $Diff_{Color}$  (the sum of  $Diff_{CVD}$  and  $ColorDiff_{NORMAL}$ ) is minimized, which is the index of the optimized line. The details are shown in the flowchart below as shown in table 3. After the index value for every representative color was calculated, the color with the lowest index value was specified as the value to be corrected, thereby identifying the optimal color.

### III. EXPERIMENTAL RESULTS

The correction method proposed in this study minimizes unnecessary color corrections because the most ideal color in the current image is selected for correction using a confusion line database during the color correction. In this way,

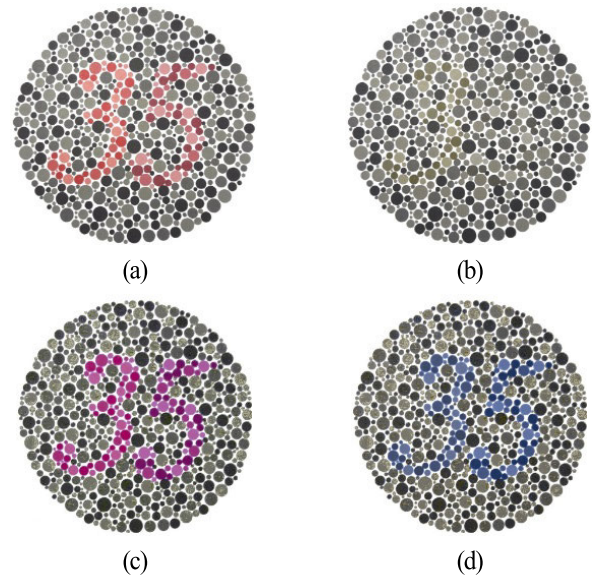


**FIGURE 17.** Experimental results of people with protanopia: (a) Original image, (b) image as perceived by those with color vision deficiency, (c) corrected image, and (d) image of (c) as perceived by those with color vision deficiency.

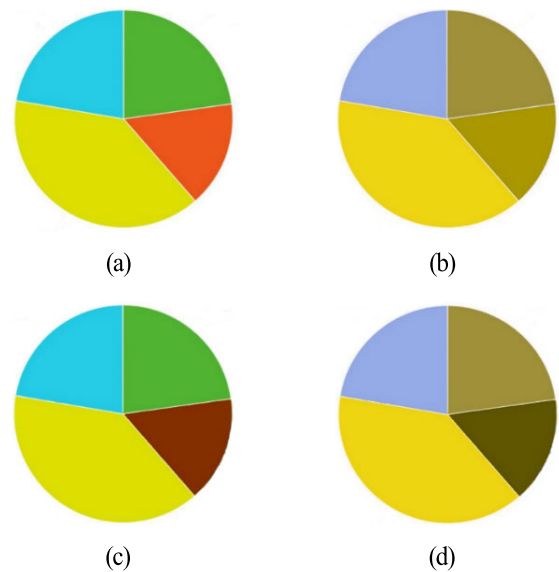


**FIGURE 18.** Experimental results of people with deuteranopia: (a) Original image, (b) image as perceived by those with color vision deficiency, (c) corrected image, and (d) image of (c) as perceived by those with color vision deficiency.

the problems of existing color correction algorithms could be overcome. For example, images corrected with the existing techniques produce improved images and color clarity for color vision deficient viewers, but from the perspective of those with normal vision, the corrected images often caused visual discomfort.

The results of various experiments on the proposed correction algorithm are presented below. As shown in figures 17, 18, and 19, the colors that color vision deficient

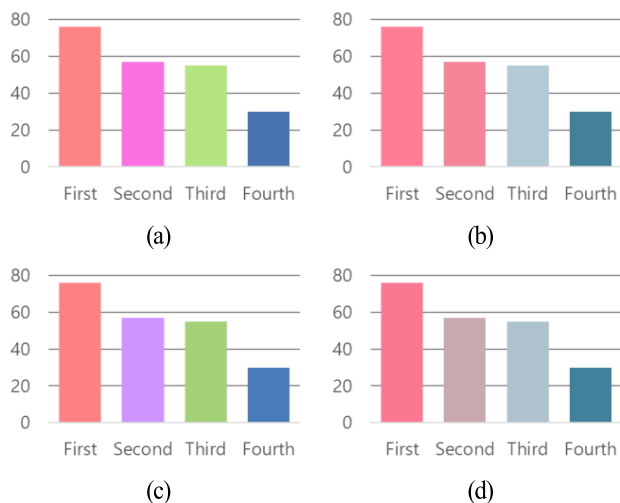


**FIGURE 19.** Experiment results of people with tritanopia: (a) Original image, (b) image as perceived by those with color vision deficiency, (c) corrected image, and (d) image of (c) as perceived by those with color vision deficiency.

people struggle to perceive were corrected in such a way as to be easily recognized and interpreted by all viewers.

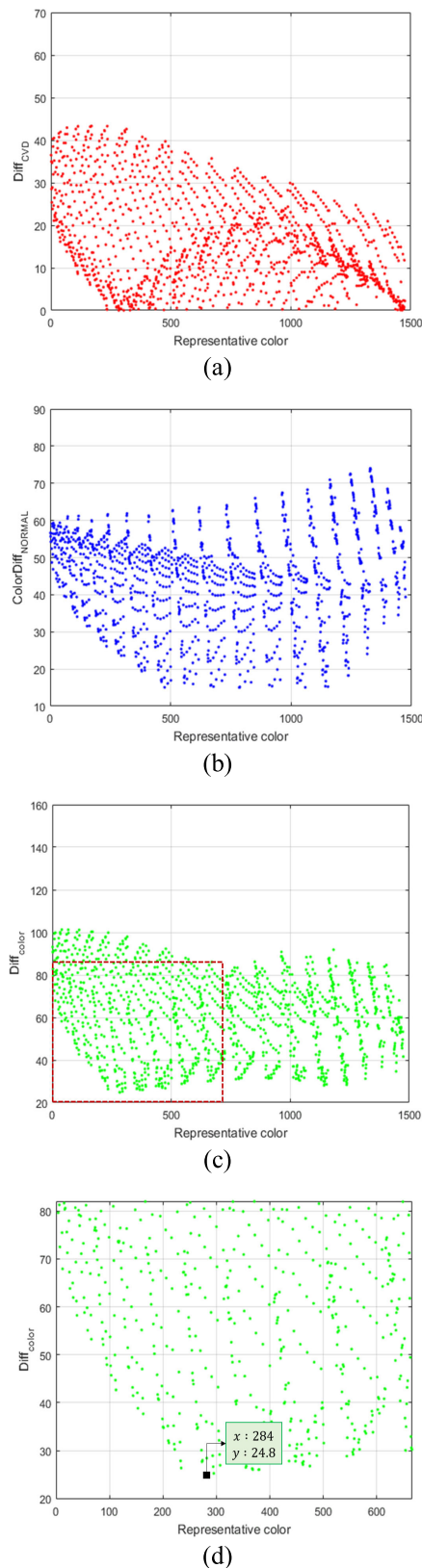
First, figure 17 shows the results of color conversion on a confusion-line based on protanopia. The normal person’s point of view (a) the number 35 is clearly identified from the background. On the other hand, the color-vision deficiency’s point of view (b) the number 35 is not distinguished from the background. The numeral region and the background exist on the same confusion line. After applying color correction using proposed method on the original image as in (c), color-vision deficiency is also divided into a numeral area and a background as shown in (d).

Figure 18 is the results of experiments in which deuteranopia looks at circular graphs. A normal person (a) clearly classifies areas of green and red into circular graphs. On the other hand, the color-vision deficiency (b) regards these areas as similar colors. If the proposed color-correction is applied, the results can be clearly differentiated by a color-vision deficiency as shown in (d).

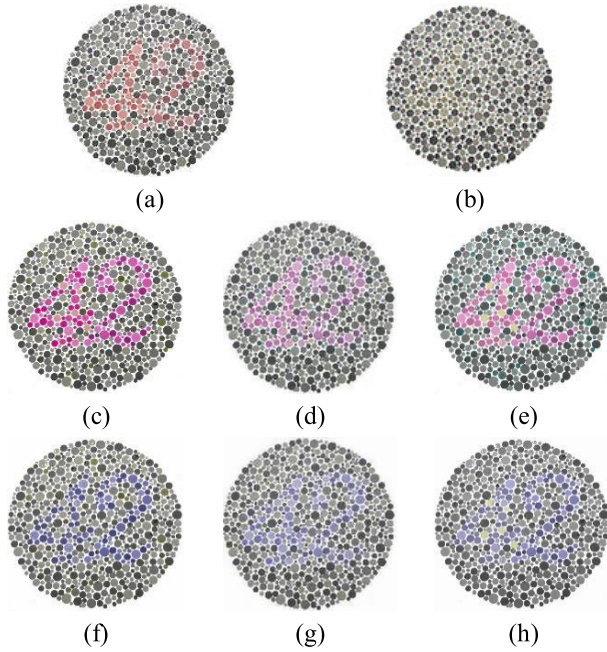
Figure 19 is the experimental results of tritanopia on circular-bar graphs. Compared to the viewpoint of a normal person (a), a color vision deficient person cannot separate the first and second rods in (b). Color correction is tried on a confusion-line, and a color-vision deficiency is also well classified in (d).

Figure 20 shows the quantitative analysis result of the circular graph in figure 18. The single part is selected on 1,475 representative colors, and (a)  $Diff_{CVD}$  and (b)  $ColorDiff_{NORMAL}$  are analyzed by a graph as follows. The selected part is a red area on a circular graph.

When the color-vision deficiency is seen, a green region and a red part cannot be differentiated on a circular graph. The smaller the color difference, the higher the probability



**FIGURE 20.** Sample of ( $Diff_{CVD}$ ,  $ColorDiff_{NORMAL}$ , and  $Diff_{Color}$  based on Chart image in figure 16: (a) Analysis result of  $Diff_{CVD}$ , (b) analysis result of  $ColorDiff_{NORMAL}$ , (c) analysis result of  $Diff_{Color}$ , and (d) enlarged analysis result of  $Diff_{Color}$ .



**FIGURE 21.** Comparison result 1 with existing studies [9] and [2]: (a) Original image, (b) image perceived by people with protanopia, (c) correction result of the proposed method, (d) correction result of [9], (e) correction result of [2], (f) image (c) perceived by people with protanopia, (g) image (d) perceived by people with protanopia, and (h) image (e) perceived by people with protanopia.

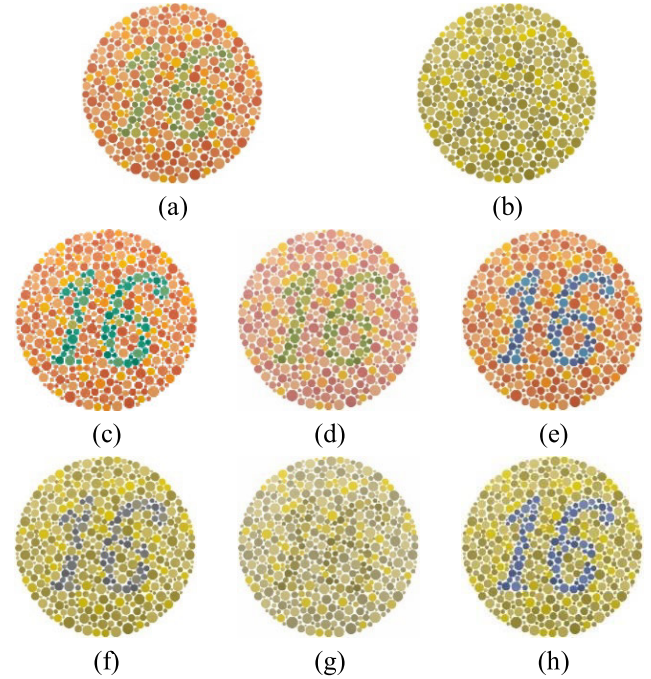


**FIGURE 22.** Comparison result 2 with existing studies [9] and [2]: (a) Original image, (b) image perceived by people with deuteranopia, (c) correction result of the proposed method, (d) correction result of [9], (e) correction result of [2], (f) image (c) perceived by people with deuteranopia, (g) image (d) perceived by people with deuteranopia, and (h) image (e) perceived by people with deuteranopia.

of indivisibility. The 1,475 pieces of such data are generated, and it selects a color to be converted while considering both the normal person and color-vision deficient person.

Figure 20(c) shows the result of measuring  $Diff_{Color}$  by using the information of  $Diff_{CVD}$  and  $ColorDiff_{Normal}$  analyzed in the previous stage. The smaller the  $Diff_{Color}$  is, the more likely it is to be closer to original as perceived by a normal person while the  $color_{val}$  in equation (4) ensures that it is clearly classified when the color-vision deficiency looks at this chart. (d) is the result of enlarging 0 ~ 750 regions within the range of 1,475, and the 284<sup>th</sup> color is the lowest difference. The color number 284 is reddish-brown, and as a result, the red color region is converted to reddish-brown on the circular graph.

The results compared with the related works [9] and [2] are shown in figure 21-22. Figures 21 and 22 show the results for protanopia and deuteranopia respectively. The isihara chart database is used for objective comparison. The normal person is clearly divided into numerical area and background. On the other hand, a color-vision deficient person cannot distinguish the number from the background as in (b). (c, d, e) shows the result of the conversion of the original image (a) into (the proposed color-correction, daltonization [9], Han's method [2]).

We can see that they all have succeeded in enabling those affected by color vision deficiency to distinguish colors that they otherwise would not typically or accurately perceive.

In an existing study [9], the confusing regions as well as other colors are corrected in such a manner that people with

normal vision experience a significant difference in color perception. In another study [2] and this study, only the regions with a small area of confused colors are corrected to minimize those potential significant differences in perception.

On the other hand, the study [2] only focuses on the perception by color vision deficient people, the corrected colors are excessively corrected, and the visual perception of those with normal vision is hardly considered. In our study, the colors were corrected so that they will not give a high sense of difference even when perceived by people with normal vision as well as by color-vision deficient person.

Figure 23 shows the experimental results for the image corresponding to S2 within figure 24. S2 image includes a variety of color spectrums, unlike images such as graphs, charts, and pies. (c) changes the color of red pepper region minimally and the pepper region of (f) clearly distinguished and perceived by color-vision deficient person. Therefore, color correction with natural images also validated. Therefore, the proposed method of this study determined the optimal color from the overall point of view. Quantitative evaluations were also performed using the seven sample images in figure 24, and the results are graphed within figure 25 to 27.

Figure 25 shows the total sum of  $ColorDiff_{NORMAL}$ , which is the difference in color data between the corresponding regions of the original image and each corrected image, to compare the color data before and after correction. The orange color region is not visible in figure 25 because the difference value between the original images is zero. Among the

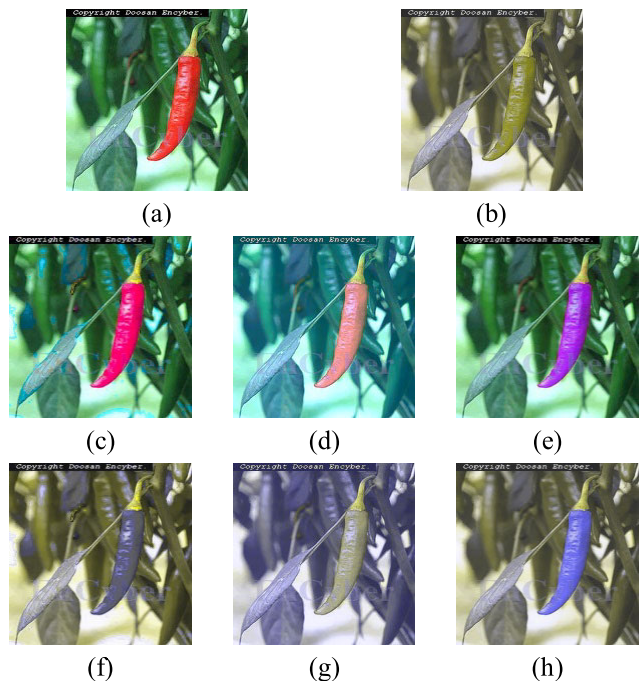


**FIGURE 23.** Comparison result of S2 with existing studies [9] and [2]: (a) Original image, (b) image perceived by people with protanopia, (c) correction result of the proposed method, (d) correction result of [9], (e) correction result of [2], (f) image (c) perceived by people with protanopia, (g) image (d) perceived by people with protanopia, and (h) image (e) perceived by people with protanopia.

correction methods, the result of this study shows the lowest value, confirming that people with normal vision experience the least color difference between the original and corrected images in the result of this study when compared to other studies.

Figure 26 shows the total sum of color differences after Brettel’s simulation in every confusing region using the  $ColorDiff_{CVD}$  value. Because the  $ColorDiff_{CVD}$  value is the result of comparison after simulation from the viewpoint of color vision deficient people, it is normal that the color difference in the simulation result after color correction is greater than the simulation result of the original image. Figure 26 shows that all color difference results of this study are greater than those of the original image. In general, it is easier to perceive color when this value is higher, but if this value becomes too large, such as in [2], most people with normal vision experience an uncomfortable difference in color perception.

The algorithm of [2] shows such data as in figure 26 because its correction feature is to simply increase blueness without considering the difference in perception sense of viewers with normal vision. Furthermore, in the sample images S3, S5, and S7, the result values of [9] are smaller than those of the original image. This case shows that the correction result of the confusing color is confused with another color, and the result of comparison with the original image may not be improved.

The comparison results of  $Diff_{Color}$ , which is an index considering the viewpoints of those with normal vision and

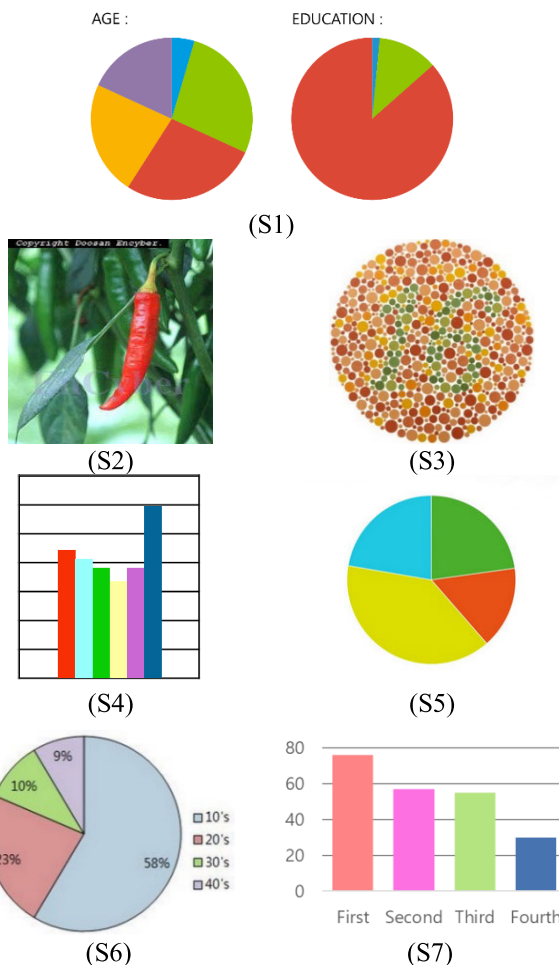


**FIGURE 24.** Images used for comparison: (S1) confusing image for people with protanopia, (S2) confusing image for people with protanopia, (S3) confusing image for people with deuteranopia, (S4) confusing image for people with deuteranopia, (S5) confusing image for people with deuteranopia, (S6) confusing image for people with tritanopia, and (S7) confusing image for people with tritanopia.

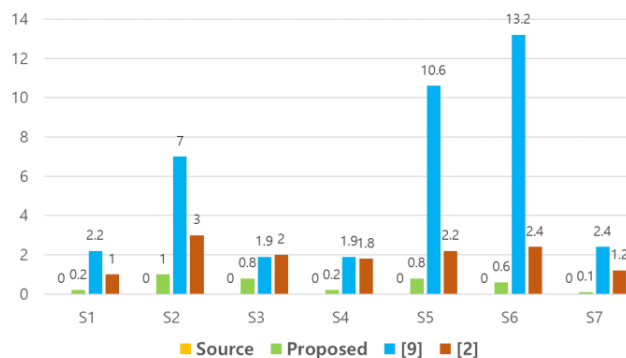


**FIGURE 25.** Comparison of  $ColorDiff_{NORMAL}$ .

color vision deficient people, is shown in figure 27. This value was obtained by adding up all of the color differences of the corresponding color regions and confusing regions while considering the original image, corrected image, and Brettel’s simulated image. We can see that the correction result of this

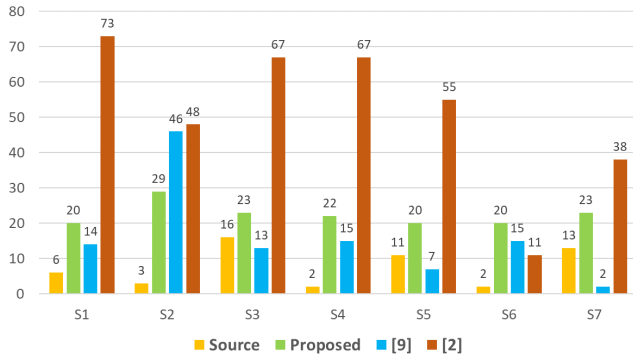


FIGURE 26. Comparison of ColorDiff<sub>CVD</sub>.

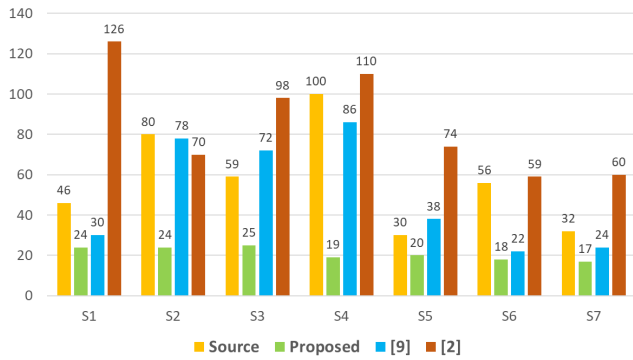


FIGURE 27. Comparison of Diff<sub>Color</sub>.

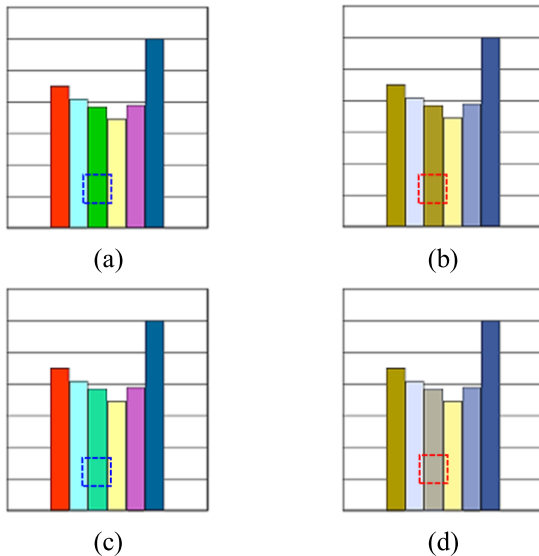


FIGURE 28. Correction example of S4 image: (a) Perception by people with normal vision, (b) perception by people with deuteranopia, (c) corrected image perceived by people with normal vision, and (d) corrected image perceived by people with deuteranopia.

study has the smallest value compared to the original image as well as compared to the results of other studies. The proposed method selected the optimal color for people with normal vision to perceive minimum color difference while allowing color vision deficient people to distinguish colors that they would otherwise not accurately perceive. A smaller value of

$Diff_{Color}$  indicates less distortion from the image for normal people, while guaranteeing clear distinction for color vision deficient people.

The original image produces a greater  $Diff_{Color}$  because  $Diff_{CVD}$  in equation (4) results in a bigger value when color vision deficient people cannot perceive the confusing region. Figure 27 exhibits the best resulting value obtained from the S4 image and its correction and simulation results for the S4 sample image are shown in Figure 28. In this case, viewers with normal vision perceive no difference before and after the color conversion, and readability and interpretation has improved greatly for color vision deficient viewers. The blue box shows that the difference between the original image and the converted image is minimized based on normal people. The red box indicates that the indistinguishable colors are clearly classified based on color-vision deficiencies.

IV. CONCLUSION

In this paper, we propose an optimal color correction technology based on image analysis for color vision deficient people. A confusion line database was constructed by classifying confusing colors according to the particular type of color vision deficiency that people experience. Then the colors within the images were classified and segmented by region, and a color-differentiating measure was developed that could improve color perception for those with color vision deficiency while also minimizing the degree of color change perceived by those with normal vision. The proposed method was validated through various experiments, and it demonstrated that this study’s correction method presented the best results compared to existing methods and other studies.

The proposed method considers the viewpoints of both color vision deficient people as well as those with normal vision. Thus, it has the advantage of being applicable to the correction of color images that are observed simultaneously by different types of viewers, such as images on TV screens. If the results of this study are successfully applied to Web browsers, video viewers, and display devices, it will greatly improve the viewing experience of people affected by color vision deficiency—people who account for 8% of the global population. Also, each color-vision deficiency (protan, deutan, tritan) includes both anomalous trichromat and dichromat. The change in the degree of color perception is small as well as; the position of confusion-line is unchanged. So, the proposed algorithm is expected to be effective even in the case of moderate anomalous trichromacy.

REFERENCES

- [1] M. P. Simunovic, “Colour vision deficiency,” *Eye*, vol. 24, no. 5, pp. 747–755, 2010.
- [2] D. Han, S. J. Yoo, and B. Kim, “A novel confusion-line separation algorithm based on color segmentation for color vision deficiency,” *J. Imag. Sci. Technol.*, vol. 56, no. 3, pp. 30501-1–30501-17, 2012.
- [3] D. Fluck. (2012). *Color Blind Essentials*. [Online]. Available: <https://www.color-blindness.com>

[4] H. Brettel, F. Viénot, and J. D. Mollon, "Computerized simulation of color appearance for dichromats," *J. Opt. Soc. Amer. A, Opt. Image Sci.*, vol. 14, no. 10, pp. 2647–2655, 1997.

[5] G. M. Machado, M. M. Oliveira, and L. A. F. Fernandes, "A physiologically-based model for simulation of color vision deficiency," *IEEE Trans. Vis. Comput. Graphics*, vol. 15, no. 6, pp. 1291–1298, Nov./Dec. 2009.

[6] G. W. Meyer and D. P. Greenberg, "Color-defective vision and computer graphics displays," *IEEE Comput. Graph. Appl.*, vol. 8, no. 5, pp. 28–40, Sep. 1988.

[7] K. Cho, J. Lee, S. Song, and D. Han, "Construction of confusion lines for color vision deficiency and verification by isihara chart," *IEIE Trans. Smart Process. Comput.*, vol. 4, no. 4, pp. 272–280, 2015.

[8] C. Rigden, "The eye of the beholder' -designing for colour-blind users," *Brit. Telecommun. Eng.*, vol. 17, pp. 291–295, Jan. 1999.

[9] P. Doliotis, G. Tsekouras, C.-N. Anagnostopoulos, and V. Athitsos, "Intelligent modification of colors in digitized paintings for enhancing the visual perception of color-blind viewers," in *Artificial Intelligence Applications and Innovations III* (IFIP International Federation for Information Processing). Apr. 2009, pp. 293–301.

[10] J.-B. Huang, C.-S. Chen, T.-C. Jen, and S.-J. Wang, "Image recolorization for the colorblind," in *Proc. IEEE Int. Conf. Acoust., Speech Signal Process. (ICASSP)*, Apr. 2009, pp. 1161–1164.

[11] G. Iaccarino, D. Malandrino, M. Del Percio, and V. Scarano, "Efficient edge-services for colorblind users," in *Proc. 15th Int. Conf. World Wide Web*, 2006, pp. 919–920.

[12] M. Ichikawa, K. Tanaka, S. Kondo, K. Hiroshima, K. Ichikawa, S. Tanabe, and K. Fukami, "Web-page color modification for barrier-free color vision with genetic algorithm," in *Proc. Genetic Evol. Comput. Conf.* Berlin, Germany: Springer, 2003, pp. 2134–2146.

[13] L. Jefferson and R. Harvey, "Accommodating color blind computer users," in *Proc. 8th Int. ACM SIGACCESS Conf. Comput. Accessibility*, 2006, pp. 40–47.

[14] W. Shen, X. Mao, X. Hu, and T.-T. Wong, "Seamless visual sharing with color vision deficiencies," *ACM Trans. Graph.*, vol. 35, no. 4, 2016, Art. no. 70.

[15] J.-Y. Jeong, H.-J. Kim, T.-S. Wang, Y.-J. Yoon, and S.-J. Ko, "An efficient re-coloring method with information preserving for the color-blind," *IEEE Trans. Consum. Electron.*, vol. 57, no. 4, pp. 1953–1960, Nov. 2011.

[16] G. Tanaka, N. Suetake, and E. Uchino, "Lightness modification of color image for protanopia and deuteranopia," *Opt. Rev.*, vol. 17, no. 1, pp. 14–23, 2010.

[17] S. Poret, R. D. Dony, and S. Gregori, "Image processing for colour blindness correction," in *Proc. IEEE Toronto Int. Conf. Sci. Technol. Humanity (TIC-STH)*, Sep. 2009, pp. 539–544.

[18] E. Navon, O. Miller, and A. Averbuch, "Color image segmentation based on adaptive local thresholds," *Image Vis. Comput.*, vol. 23, no. 1, pp. 69–85, 2005.

[19] Z. Kato, "Segmentation of color images via reversible jump MCMC sampling," *J. Image Vis. Comput.*, vol. 26, no. 3, pp. 361–371, 2008.

[20] Y.-S. Chen and Y.-C. Hsu, "Computer vision on a colour blindness plate," *Image Vis. Comput.*, vol. 13, no. 6, pp. 463–478, 1995.

[21] R. Adams and L. Bischof, "Seeded region growing," *IEEE Trans. Pattern Anal. Mach. Intell.*, vol. 16, no. 6, pp. 641–647, Jun. 1994.

[22] *CIE L\*a\*b\**. Accessed: Aug. 2019. [Online]. Available: <http://www.colorbasics.com/ColorSpace/>

[23] G. Sharma, W. Wu, and E. N. Dalal, "The CIEDE2000 color-difference formula: Implementation notes, supplementary test data, and mathematical observations," *Color Res. Appl.*, vol. 30, no. 1, pp. 21–30, 2005.

[24] J. A. Hartigan and M. A. Wong, "Algorithm AS 136: A k-means clustering algorithm," *Appl. Statist.*, vol. 28, no. 1, pp. 100–108, 1979.

[25] J. A. K. Suykens and J. Vandewalle, "Least squares support vector machine classifiers," *Neural Process. Lett.*, vol. 9, no. 3, pp. 293–300, Jun. 1999.

[26] Z. Wang, A. C. Bovik, H. R. Sheikh, and E. P. Simoncelli, "Image quality assessment: From error visibility to structural similarity," *IEEE Trans. Image Process.*, vol. 13, no. 4, pp. 600–612, Apr. 2004.

[27] Q. Huynh-Thu and M. Ghanbari, "Scope of validity of PSNR in image/video quality assessment," *Electron. Lett.*, vol. 44, no. 13, pp. 800–801, Jun. 2008.

[28] T.-Y. Shih, "The reversibility of six geometric color spaces," *Photogramm. Eng. Remote Sens.*, vol. 61, no. 10, pp. 1223–1232, Oct. 1995.

[29] D. Han, "Real-time color gamut mapping method for digital TV display quality enhancement," *IEEE Trans. Consum. Electron.*, vol. 50, no. 2, pp. 691–698, May 2004.



**JONGHO CHOI** received the B.S. degree in electronics and computer engineering from Sangji University, Wonju, South Korea, in 2009, and the M.S. degree from the Department of Computer Science and Engineering, Sejong University, Seoul, South Korea, in 2011, where he is currently pursuing the Ph.D. degree with the Department of Computer Engineering. His research interests include image processing, signal processing, and computer vision.



**JUSUN LEE** received the B.S. degree in computer engineering from Sejong University, Seoul, South Korea, in 2015, and the M.S. degree from the Department of Computer Science and Engineering, Sejong University, in 2017. His research interests include image processing, signal processing, and computer vision.



**HYEONJOON MOON** received the B.S. degree in electronics and computer engineering from Korea University, in 1990, and the M.S. and Ph.D. degrees in electrical and computer engineering from the State University of New York at Buffalo, in 1992 and 1999, respectively. From January 1996 to October 1999, he was a Senior Research in Electro-Optics/Infrared Image Processing Branch with the U.S. Army Research Laboratory (ARL), Adelphi, MD, USA. He developed a face recognition system evaluation methodology based on the Face Recognition Technology (FERET) program. From November 1999 to February 2003, he was a Principal Research Scientist at Viisage Technology, Littleton, MA, USA. He has extensive background on still image and real-time video-based computer vision and pattern recognition. Since March 2004, he has been with the Department of Computer Science and Engineering, Sejong University, where he is currently a Professor and the Chairman. His current research interests include research and development in on real-time facial recognition system for access control, surveillance, big database applications, image processing, biometrics, artificial intelligence, and machine learning.



**SEONG JOON YOO** received the M.E. degree in electrical engineering from Korea University and the Ph.D. degree in computer and information science from Syracuse University. He is currently a Professor with the Department of Computer Engineering, Sejong University, Seoul, South Korea. He is also the Director of the Advanced Bigdata Center for Research and Collaboration (ABRC) and involved in the research of big data and artificial intelligence.



**DONGIL HAN** received the B.S. degree in electronics and computer engineering from Korea University, Seoul, South Korea, in 1988, and the M.S. and Ph.D. degrees in electrical and electronics engineering from the Korea Advanced Institute of Science and Technology, Seoul, in 1990 and 1995, respectively. From 1995 to 2003, he was the Chief Research Engineer with Digital TV Research and Development Laboratories, LG Electronics Inc., Seoul. He is currently a Professor with the Department of Computer Science and Engineering, Sejong University, Seoul. His research interests include image processing, display quality enhancement for digital TV, system on chip, and robot vision.

...